

## DTI using modulated gradients at short effective diffusion times

Henrik Lundell<sup>1</sup>, Casper Kaae Sønderby<sup>1</sup>, Lise Vejby Søgaard<sup>1</sup>, and Tim Bjørn Dyrby<sup>1</sup>

<sup>1</sup>Copenhagen University Hospital Hvidovre, Danish Research Centre for Magnetic Resonance, Hvidovre, Copenhagen, Denmark

**INTRODUCTION:** We investigate the effect of short effective diffusion times in rotationally invariant diffusion tensor metrics of distinct white matter structures in fixed tissue using a modulated gradient sequence. Using well-designed alternating gradient waveforms, components of the temporal diffusion spectrum can be selectively estimated and the diffusion properties over very short time and length scales can thereby be assessed. This is in contrast to ADC/DTI or *q*-space derived analysis of pulsed gradient spin echo (PGSE) or stimulated echo (STEAM) data, where the signal attenuation depends on long term diffusion processes over the full length of the diffusion encoding pulses and interference between geometry and the *q*-vector [Callaghan 1996]. Rapidly modulated gradient waveforms, such as oscillating gradient spin echo (OGSE), can provide insight into the diffusion processes in cellular microenvironments which are out of reach in conventional diffusion experiments [Gore et al 2010]. It has recently been shown that the diffusion tensor reconstructed from OGSE data with multiple gradient directions provides an additional anatomically relevant contrast in different regions of the mouse brain [Aggarwal et al 2011]. In this study a perfusion fixed Vervet monkey brain was imaged using trapezoidal modulated gradients applied in multiple directions to provide diffusion tensor imaging (DTI) data over a range of short effective diffusion times. We found an apparent reduced effect of restricted diffusion in white matter both parallel and perpendicular to the axonal direction at short diffusion times but overall maintained anisotropy and new anisotropic structures emerged at the gray/white matter border visible at short diffusion times only.

**METHODS: Gradient waveform design:** Modulated gradients were constructed of multiple bipolar trapezoidal gradient pulses on each side of the 180°-pulse with two half length pulses placed in the beginning and at the end of the pulse train as shown in figure 1A. The half pulses remove the zero frequency component in the spectral domain of *f(t)* (see figure 1B where *g*\*(*t*) denotes the effective gradient inverted by all prior refocusing pulses) and hence the sensitivity to the low frequency domain of the temporal diffusion spectrum, i.e. disperse flow and long term diffusion components, similar to the cosine modulated OGSE [Stepisnik et. al. 2001, Parsons et al, 2003]. We varied the modulating frequency by changing the gradient separation ( $\Delta$ ) but kept the *q*-value constant (fixed maximum gradient strength (*G*) and duration ( $\delta$ )). The number of loops (*N*) was maximized within the two RF-silent periods around the 180°-pulse. Gradient waveforms were designed using an in-house developed Matlab/Scanner-interface.

**Brain tissue sample:** A 32 month normal Vervet monkey brain was prepared for post mortem imaging as described earlier [Dyrby et al 2011]. The left hemisphere was removed ~5 mm lateral to the sagittal midline of corpus callosum. All procedures for handling experimental animals followed ethical guidelines approved by relevant authorities.

**Imaging:** Data was acquired on a Varian 4.7 T preclinical scanner using a home built 19 mm diameter surface coil placed on the sagittal surface proximal to the corpus callosum. Image were acquired using a conventional single line spin-echo readout with voxel size 0.5x0.5x1.5 mm<sup>3</sup>, 7 slices, TR=3000 ms and TE=96 ms. *G* and  $\delta$  were fixed to 0.32 Tm<sup>-1</sup> and 3.5 ms, including a rise time of 1.6  $\mu$ s resulting in *q*=(44  $\mu$ m)<sup>-1</sup>. Gradient separation ( $\Delta$ ) was varied from 3.5 to 6 ms in steps of 0.25 ms, *N* was [4 4 4 4 3 3 3 3 2 2 2] for the respective 11 increments of  $\Delta$  giving 4(*N*+1) diffusion encoding periods in *f(t)*. The gradient (*G*) was applied in 20 non-collinear directions obtained from an electrostatic pointset [Jones et al 1999] and low *b*-value reference scans were acquired for each gradient direction with the gradient strength *G*=0.1 Tm<sup>-1</sup>. The magnet bore temperature was stabilized with a constant airflow and monitored during the whole experiment [Dyrby et al 2011]. The protocol was repeated twice and the analysis was performed on averaged datasets (SNR of ~50 for low *b*-values in white matter).

**Data analysis:** The *b*-matrix of the whole gradient train was estimated by numerical integration of gradient amplifier input time series and the diffusion tensor was estimated using linear fitting in the Camino toolbox [Basser et al, 1996, Cook et al 2006]. Parallel diffusivity was expressed as the primary eigenvalue  $D_{\text{par}}=\lambda_1$  and perpendicular diffusivity was  $D_{\text{perp}}=(\lambda_2+\lambda_3)/2$ . The diffusion time is not well defined for finite pulse durations but we expressed the effective diffusion time relative to the *b* value of the single diffusion encoding blocks of *f(t)* and found  $\tau_{\text{eff}}=b/q^2$  ranging from 1.3 to 3.8 ms [Gross and Kossfeld, 1968].

**RESULTS & DISCUSSION:** An ROI was drawn in the mid-sagittal section covering the corpus callosum and tensor parameters were extracted from this region (fig. 2A). As expected, clear increases in both parallel and perpendicular diffusivities were observed at decreased effective diffusion times indicating the decreased effect of restrictions. The effect on  $D_{\text{par}}$  suggests that diffusivity along the axons has hindered or restricted components. Those could have microscopic origin, such as intra-axonal structures or cell bodies in the extra-axonal space, but may also be due to macroscopic effects like dispersion or bending fibers over the relatively thick slice.

The color coded FA-maps outlined the main white matter pathways in the scanned region with overall appearance maintained down to the shortest effective diffusion time, as seen in the sagittal section ~3 mm lateral to the mid-plane shown in figure 2B. Anisotropy was also observed in one consistent layer in cortical gray matter ordered in a radial fashion (Fig 2B, white arrows) as observed at longer effective diffusion times in PGSE experiments [Dyrby et al 2011].

Moreover and interestingly, new anisotropic structures perpendicular to the original principal direction at long diffusion times emerged at short effective diffusion times in white matter along the gray matter border, (fig 2B, green arrows). The emerged anisotropic structures were found consistently along the gray/white matter border but only at shorter  $\tau_{\text{eff}} < 2$  ms. Thin fibers entering gray matter becoming the dominant anisotropic compartment compared to a main fasciculus with larger diameter axons could explain this observation. However, further investigations are needed to confirm this finding.

**CONCLUSION:** This study shows the feasibility of investigating unrestricted diffusion with DTI at short effective diffusion times in brain tissue using trapezoidal modulated gradients. Trapezoidal or square gradients may not provide optimal temporal spectral specificity compared to OGSE but introduces mainly higher unrestricted frequency components and allow a factor  $\pi/2$  higher *q*-value for a given maximum gradient strength and thus higher *b*-weighting and better contrast to noise which is a limiting factor of relevance for potential human *in vivo* applications.

**REFERENCES:** Callaghan (1996) Oxford University Press, Gore et al (2010) NMR Biomed, Basser, et al (1994), JMRI, Cook, P. A., et al (2006), in proc. ISMRM, Gross and Kossfeld (1968), Messtechnik, Stepisnik et al. (2001) Physica B, Aggarwal et al (2011) MRM, Dyrby et al. (2011), HBM, Jones et al. (1999) MRM.

**ACKNOWLEDGEMENTS:** The future and emerging technologies (FET) program of the EU FP7 framework funds the CONNECT consortium and supports this work.

**Figure 1**

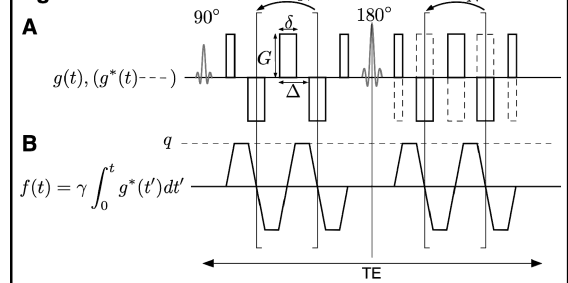


**Figure 2**

